High Pressure Research, 2002, Vol. 22, pp. 127–130

Taylor & Francis
Taylor & Francis Group

OPTICAL SPECTROSCOPIC STUDY OF Al_2O_3: Ti^{3+} UNDER HYDROSTATIC PRESSURE

S. GARCÍA-REVILLA[a,*], F. RODRÍGUEZ[a], I. HERNÁNDEZ[a], R. VALIENTE[a] and M. POLLNAU[b]

[a]*DCITIMAC, Facultad de Ciencias, Universidad de Cantabria, Santander 39005, Spain;* [b]*Institute of Applied Optics, Department of Microtechnique, Swiss Federal Institute of Technology, CH-1015 Lausanne, Switzerland*

(Received 13 July 2001; In final form 29 September)

This work investigates the effect of hydrostatic pressure on the excitation, emission and lifetime of Ti^{3+}-doped Al_2O_3 in the 0–110 kbar range. The application of pressure induces band shifts that are correlated with the corresponding local structural changes undergone by the TiO_6 complex. The increase of the Stokes-shift and the reduction of the Jahn–Teller (JT) splittings under pressure are analysed in terms of a simple model based on linear electron–phonon couplings to the a_{1_g} and the JT e_g vibrational modes.

Keywords: Jahn–Teller Effect; Al_2O_3:Ti^{3+}; Hydrostatic pressure; Optical spectroscopy

1 INTRODUCTION

The technological application of NIR tunable lasers has motivated the fundamental study of transition metal ions such as Ti^{3+}, Ni^{2+}, Cr^{2+}, Cr^{4+} or Mn^{5+}. Among them, Ti^{3+} is the ion with the simplest electronic configuration, $3d^1$. When this ion is introduced into Al_2O_3, the C_{3v} crystal field (nearly octahedral) splits the ^2D free ion state into ^2E_g and $^2T_{2g}$ states. Although Al_2O_3:Ti^{3+} has been intensively investigated for its extraordinary laser capabilities, there are fundamental aspects concerning electron–phonon coupling, which deserves clarification. This fact together with the Jahn–Teller (JT) character of Ti^{3+} makes it very attractive system as a four-level laser material (Fig. 1). This work investigates the variation of the linear electron–phonon couplings between ^2E_g and $^2T_{2g}$ electronic states, and the a_{1g} and JT e_g vibrational local modes as a function of the crystal volume (*i.e.* $Ti^{3+}-O^{2-}$ distance). For this purpose, we have carried out excitation, luminescence and lifetime measurements under hydrostatic pressure in the 0–110 kbar range. Previous pressure works on Al_2O_3:Ti^{3+} by optical absorption spectroscopy [1] and luminescence at low temperature [2] were not done in purely hydrostatic conditions, what is a serious impediment to achieve this goal.

* Corresponding author.

ISSN 0895-7959 print; ISSN 1477-2299 online
DOI: 10.1080/08957950290003085

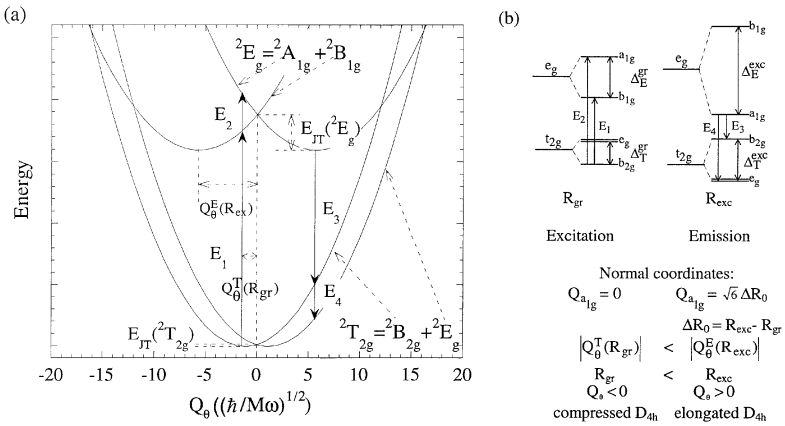

FIGURE 1 (a) Configurational-coordinate potential-energy diagrams of the ^2E_g and $^2T_{2g}$ electronic states for the TiO_6 complex. E_1 and E_2 (E_3 and E_4) indicate the electronic transitions between the ground-state (excited-state) minimum and the excited (ground) state. (b) One-electron energy level diagrams illustrating the absorption and emission transitions. The splittings correspond to the Jahn–Teller effect in the ground state (left) and in the excited-state (right).

2 EXPERIMENT

Microcrystals of Al_2O_3 doped with 0.35 mol% Ti^{3+} ($\sim 50 \times 120 \times 70\,\mu m^3$), grown by the Kyropoulos technique, were studied by hydrostatic pressure experiments using a diamond anvil cell (High Pressure Diamond Optics, Inc.). A mixture of 16:3:1 methanol–ethanol–water was used as pressure transmitter medium. The 530.9 nm line of a Kr^+-ion laser (Coherent CR-500 K) was used to pump the Ti^{3+} into the ^2E_g excited state. We used a Jobin-Yvon U1000 double-monochromator for the emision spectra, while the excitation spectra were obtained by means of a photoluminescence setup specially designed for detecting very weak intensities. For lifetime measurements the excitation beam was modulated with an acousto-optic modulator and the signal processing was accomplished by Tektronix 2430 A digital scope. The pressure was calibrated through the Raman shift of Silicon chips in order to prevent unwanted luminescence signal from Ruby chips (see more details in ref. [3]).

3 RESULTS

Figure 2(a) shows the luminescence and corresponding excitation spectra of Al_2O_3:0.35 mol% Ti^{3+} at ambient conditions. Both spectra consist of a broad band exhibiting a double-humped structure, which is mainly associated with the JT effect. The variation of the transition energy upon pressure is plotted in Fig. 2(b). The splittings related to the JT effect and the trigonal crystal-field components for excitation and emission are respectively given by

$$\Delta^{gr}_E(P) = E_2 - E_1 = 2900 - 1.66\,P$$
$$\Delta^{exc}_T(P) = E_4 - E_3 = 1220 - 0.53\,P$$

The $\Delta^{gr}_E(P)$ and $\Delta^{exc}_T(P)$ splittings correspond to an average Ti^{3+}–O^{2-} distance R_{gr} for the ground state and R_{exc} for the excited state. The splittings decrease both upon increasing

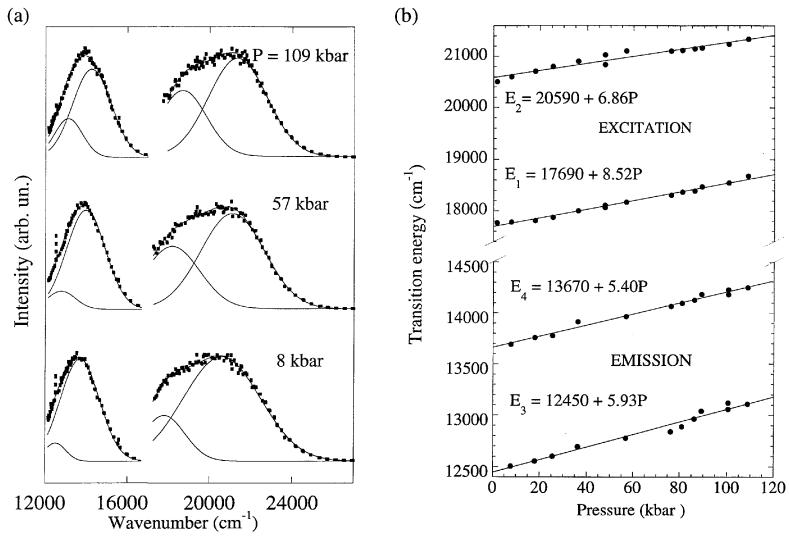

FIGURE 2 (a) Variation of the emission and excitation spectra with hydrostatic pressure at $T = 293$ K. All the spectra have been fitted to the sum of two gaussians. Solid lines represent the gaussians and the corresponding sums, together with the experimental data (dots). (b) Emission and excitation shifts corresponding to the peak energy of the two components of the luminescence and excitation spectra. Straight lines are linear fits of the data.

the pressure. On the other hand, the variation of the centroid of the bands, directly related to 10 Dq, increases by 7.7 cm^{-1}/kbar with the pressure, as it is expected for a reduction of the Ti^{3+}–O^{2-} distance.

4 DISCUSSION

The emission and excitation spectra at ambient pressure and room temperature of Al_2O_3:Ti^{3+}, can be explained on the basis of simple octahedral TiO_6 complex, through linear electron–phonon couplings between the $^2T_{2g}$ electronic ground state (for excitation) and the ^2E_g electronic excited-state (for emission) with the totally symmetric a_{1g} and the JT e_g (Q_θ, Q_ϵ) vibrational local modes [4]. Within this scheme two transitions are possible for excitation (E_1 and E_2) and also for emission (E_3 and E_4) (Fig. 1). The corresponding splitting shown in Fig. 1(b) gives directly the JT distortion of the complex in their respective ^2E_g and $^2T_{2g}$ electronic states (Δ_E^{gr} $(R_{gr}) = 2740\,cm^{-1}$ for excitation, and Δ_T^{exc} $(R_{exc}) = 1540\,cm^{-1}$ for emission). It is noteworthy that these splittings are similar although the electron–phonon coupling of the ^2E_g octahedral state for the same value of the configuration coordinate, Q_θ, is about four times higher than for $^2T_{2g}$ [5, 2]. Within a linear electron–phonon coupling to e_g vibration, the JT splittings can be expressed as [3]

$$\Delta_T^{exc}(R_{exc}) = |A_1^T Q_\theta^E| = \frac{A_1^T A_1^E}{K_{exc}} \quad \text{and} \quad \Delta_E^{gr}(R_{gr}) = |A_T^E Q_\theta^T| = \frac{A_1^E A_1^T}{K_{gr}}$$

Here, $K_i = \mu \cdot \omega_i^2$ is the force constant for the e_g vibration and ω_i is the corresponding angular frequency with $i =$ gr and exc for the parent octahedral ^2E_g and $^2T_{2g}$ electronic

states, respectively. The total contributions to the Stokes-shift including both JT e_g and a_{1g} couplings are: $E_{SS}^{JT} \equiv \frac{1}{2}[|A_1^E Q_\theta^E| + \frac{4}{3}|A_1^T Q_\theta^T|]$ and $E_{SS}(a_{1g}) = |A_{a_{1g}} Q_{a_{1g}}|$, where $A_{a_{1g}} = (\partial 10\,Dq/\,\partial Q_{a_{1g}})_{Q_{a_{1g}}=0}$. These values can be measured independently as a function of the crystal volume by optical spectroscopy under pressure. Figure 2 shows that the JT splittings decrease under pressure, while the Stokes-shift contribution for a_{1g} increases.

Assuming variations of the linear electron–phonon coupling with volume (or R) as $A_{a_{1g}} \propto R^{-(n+1)}$ with $n = 5$ for oxides [1] and $\omega_{a_{1g}} \propto R^{-3\gamma}$, then $Q_{a_{1g}} \propto R_{gr}^{-6(1-\gamma)}$, thus $E_{SS}(a_{1g}) \propto R^{-6(2-\gamma)}$. Taking $\gamma \approx 1.31$ [6], we can justify why Stokes-shift increases upon increasing the pressure. On the assumption that $A_1^T \propto R_{gr}^{-(n_T+1)}$ and $A_1^E \propto R_{exc}^{-(n_E+1)}$, we obtain, analogously, the JT splitting as a function of the ground- and the excited-state equilibrium geometries, R_{gr} and R_{exc}, are given by:

$$\Delta_E^{gr}(R_{gr}) \propto \frac{R_{gr}^{-(n_E+1)} R_{gr}^{-(n_T+1)}}{\omega_{gr}^2} \quad \text{and} \quad \Delta_T^{exc}(R_{exc}) \propto \frac{R_{exc}^{-(n_T+1)} R_{exc}^{-(n_E+1)}}{\omega_{exc}^2}$$

where $R_{exc} = R_{gr} + \Delta R$ and $n_E < n_T$. Taking $10\,Dq = 19130\,cm^{-1}$, $\hbar\omega_{a_{1g}} = 515.3\,cm^{-1}$ [7] and $R_{gr} = 1.9$ Å, then we estimate $R_{exc} = 2.06$ Å at $P = 0$. Vibrational energies for TiO_6 in Ti^{3+}:Al_2O_3 are: $\hbar\omega_T = 239\,cm^{-1}$ and $\hbar\omega_E \approx 200\,cm^{-1}$ [4]. Using $n_T = n_E = 4$, we find a relationship between their corresponding JT splittings as

$$\frac{\Delta_E^{gr}(R_{gr})}{\Delta_T^{exc}(R_{exc})} \equiv \left(\frac{R_{gr}}{R_{exc}}\right)^{-(n_E+n_T+2)} \left(\frac{\omega_{exc}}{\omega_{gr}}\right)^2 = 1.57,$$

which is very similar to the observed value of $(\Delta_E^{gr}(R_{gr})/\Delta_T^{exc}(R_{exc})) = 2740/1530 \sim 1.8$.

However, the situation is rather different for the pressure dependence of the JT splitting, which decreases with the pressure (Fig. 2(b)). Considering $\Delta_E^{gr}(R_{gr}) \propto A_1^E A_1^T \omega_{gr}^{-2} \propto R_{gr}^{-(10-6\gamma')}$, a decrease of the JT splitting induced by pressure can be explained through this model provided that $\gamma' > 1.7$, for the e_g local mode.

In conclusion, the opposite pressure behaviour exhibited by the Stokes-shift and the JT splittings associated with the ^2E_g and $^2T_{2g}$ electronic states, can be explained in terms of a simple TiO_6 octahedral model, considering linear electron–phonon coupling to the local a_{1g} and the JT e_g vibrational modes. The distinct pressure behaviour is mainly associated with a different Grüneisen parameter for each mode: $\gamma_{a_{1g}} < 1.7$ and $\gamma_{e_g} > 1.7$.

A complete analysis of the present results is given elswhere [3].

Acknowledgements

We are indebted to the Vicerrectorado de Investigación of the University of Cantabria and the CICYT (Project No PB98-0190) for financial support.

References

[1] Minomura, S. and Drickamer, H. G. (1961). *J. Chem. Phys.*, **35**, 903.
[2] Jia, W., Liu, H., Lim, K. and Yen, W. M. (1989).*J. Lumin.*, **43**, 323.
[3] García-Revilla, S., Rodríguez, F., Valiente, R. and M. Pollnau, M. (2002) *J. Phys.: Condens. Matt.* **14**, 447.
[4] Grinberg, M., Mandelis, A. and Fjeldsted, K. (1993). *Phys. Rev. B*, **48**, 5935; Grinberg, M., Mandelis, A., Fjeldsted, K. and Othonos, A. (1993). *Phys. Rev. B*, **48**, 5922.
[5] Valiente, R. and Rodríguez, F. (1999). *Phys. Rev. B*, **60**, 9423.
[6] Watson, G. H., Jr. and Daniels, W. B. (1981). *J. Appl. Phys.*, **52**, 956.
[7] Sekiya, T., Ohta, S., Kamei, S., Hanakawa, M. and Kurita, S. (2001). *J. Phys. Chem. Solids*, **62**, 717.